Arabian Journal for Science and Engineering (2022) 47:6155–6166
https://doi.org/10.1007/s13369-021-06014-7

RESEARCH ARTICLE-CHEMICAL ENGINEERING

Adsorption of Nickel(II) Ions from Synthetic Wastewater Using Activated Carbon Prepared from *Mespilus germanica* Leaf

Ali Khedri[1] · Dariush Jafari[2] · Morteza Esfandyari[3]

Received: 26 January 2021 / Accepted: 14 July 2021 / Published online: 27 July 2021

Abstract
Today one of the major environmental issues is the contamination of surface waters by toxic heavy metals. Such pollutants cannot be decomposed in environment and jeopardize human health. Therefore, the removal of these ions from water and wastewater has been considered as a worldwide concern. In this work, the activated carbon which was produced from *Mespilus germanica* leaf was used for the removal of Ni^{2+} ions from aqueous solution, and the effect of operating parameters, namely solution pH (3–10), the dosage of adsorbent (0.1–0.7 g/L), contact time (10–80 min), process temperature (298–348 K), and nickel ion initial concentration (10–70 ppm) were investigated on its adsorption percentage. Additionally, the prepared adsorbent was characterized by BET, SEM, XRD, FTIR, and EDAX techniques. Based on the results of BET analysis, the surface area of the adsorbent was 10.39 m^2/g. The optimal nickel ions adsorption efficiency was 97.56% which was achieved in the following optimal operating conditions: pH = 7, adsorbent dosage = 0.4 g/L, contact time = 50 min, 298 K, and nickel ion initial concentration = 60 ppm. In addition, the equilibrium and kinetic investigations showed that Langmuir isotherm and the pseudo second-order kinetic models described the equilibrium behavior and kinetics of the current adsorption process well. Langmuir isotherm data showed that the maximum adsorption capacity was equal to 13.08 mg/g. Additionally, the thermodynamic study of the process indicated that Ni^{2+} ions adsorption by the produced activated carbon was exothermic.

Keywords Adsorbent · Nickel ion · *Mespilus germanica* leaf · Adsorption · Aqueous solution · Activated carbon

1 Introduction

As a result of development of industries, various harmful pollutants are emitted in environment which potentially increase the health risks. Environmental protection organizations have categorized the heavy metals ions including cadmium, nickel, chrome, copper, and mercury as the dangerous environmental toxic pollutants. These pollutants, which cannot be simply decomposed, have been emitted in environment by wastewater of industries such as plating, photography, aerospace, atomic energy, and petrochemical facilities. These chemicals pollute the environmental ecologies such as surface waters, agriculture products, and human body and increase the risk of diseases in different body organisms like brain, skin, liver, pancreas, and heart [1, 2]. Nickel is one of these toxic non-decomposable metallic species which is introduced into environment by the wastewater of industries such as steel, batteries, and electronics [3, 4]. Researchers have always focused on the removal of such metals from the water and wastewater of industries using several techniques like chemical deposition, electric coagulation, reverse osmosis, electrochemical methods, and the application of ion exchange resins [5]. The above mentioned techniques have some disadvantages like sedimentation and low capacities and low efficiencies. Additionally, they require a permanent control strategy. Because of all of the mentioned defects, the application of effective techniques with high efficiencies and low cost of operation for the uptake of heavy metal pollutants is increasingly recognized as a serious worldwide requirement. Several advantageous features such as low cost operation, simplicity, acceptable efficiency, capability of the

✉ Dariush Jafari
dariush.jafari@yahoo.com

[1] Department of Chemical Engineering, Dashtestan Branch, Islamic Azad University, Bushehr, Iran

[2] Department of Chemical Engineering, Bushehr Branch, Islamic Azad University, Bushehr, Iran

[3] Department of Chemical Engineering, University of Bojnord, Bojnord, Iran

adsorbent recovery, and reasonable removal rate have made the adsorption as a major area of interest within the field of treatment of wastewaters polluted by heavy metal ions [6]. The low cost of adsorption operation can be attributed to the possibility of production of activated carbon-based adsorbents from agricultural wastes. Some of such waste products which have been used for this purpose are pieces of pat woods, charcoal, coconut shell, and fruit and nut peel. As a result of recent developments in the field of adsorption process, preparation of low-cost activated carbon-based adsorbents for the treatment of wastewaters include heavy metals has received renewed interest [7]. Several properties of the prepared adsorbents such as porosity and chemical structure affect their adsorption capability, since these features influence the interactions between polar and nonpolar pollutants and the adsorbent's active sites directly [8].

The adsorption of heavy metals from aqueous systems by activated carbon-based adsorbents produced from the different plant components has been the object of many researches. Some of the applied adsorbents are prepared from date stones [9], pistachio shell [10], pecan nutshell [11], honeydew peels [12], *Citrus limetta* [13], and waste potato peels [14] and were used for removal of heavy metal ions from wastewater. Despite the high number of studies related to this field, the development of appropriate adsorbents is still necessary.

The central thesis of this paper is the application of an activated carbon-based adsorbent derived from the leaf of the *Mespilus germanica* in order to remove nickel(II) ions from aqueous solutions. Additionally, the produced activated carbon was analyzed through BET, SEM, XRD, FTIR, and EDAX techniques. The significance of operating variables namely solution pH, dosage of adsorbent, contact time, temperature, and nickel ion initial concentration were examined with respect to removal efficiency of nickel(II) ion. Langmuir and Freundlich isotherms were applied to describe the equilibrium behavior of the adsorption process. In addition, the kinetic investigations were done by pseudo-first-order and second-order kinetic models, and enthalpy, entropy, and Gibbs free energy were studied in various temperatures to evaluate the thermodynamic behavior of the process.

2 Materials and Methods

2.1 Chemicals

In this work, the wastes of gardens in Bushehr province (Iran) were used as the source of leaves of *Mespilus germanica* for the preparation of the activated carbon. Nickel(II) nitrate ($Ni(NO_3)_2$) was purchased from Merck company (Germany) and used as received. In order to adjust the solution pH, HCl and NaOH were purchased (Merck Co., Germany) and were used as received. Additionally, the solutions containing nickel(II) ions were prepared by double-distilled water.

2.2 Preparation of Activated Carbon

As the initial step, the collected leaves were washed by double-distilled water to remove dust and other impurities. Afterward, they were placed in an oven for 120 min at 100 °C to be dried completely. Then, the dried leaves were placed in a vacuum furnace at the temperature of 550 °C for about 180 min to convert into carbon. The achieved carbon was grinded using an electric grinder and graded by sieve No. 25 (ASTME11) to prepare activated carbon for further use as the adsorbent.

2.3 Equipment and Instruments

A flame atomic adsorption device (Young lin, model AAS-8020) was used for the measurement of the residual nickel ion concentration in aqueous solutions after adsorption. Additionally, Metrohn digital pH meter was used to measure the pH of solutions. The activated carbon's surface functional groups and their variations after the adsorption were determined using Bomem MB-series FTR spectrometer. Moreover, the surface structure and the morphology of the activated carbon were studied by SEM TESCAN, while the crystalline phases of the adsorbent were characterized by a GNR MPD 3000 XRD device. Furthermore, the elements present in the adsorbent structure were determined using EDAX analysis (Philips-x130), and its surface area was measured by BET device (SAP2020A).

2.4 Preparation of Stock Solution and Adsorption Experiments

In order to synthesize the stock solution of nickel(II) ions an accurately weighted amount of nickel(II) nitrate was dissolved in double-distilled water in a 100-mL beaker. The desired concentrations of nickel ion was then prepared by dilution of the prior solution. Additionally, pH of the solutions for the adsorption tests were adjusted using 1 M HCl and 1 M NaOH.

Nickel(II) ions batch adsorption experiments were performed by varying the parameters included solution pH (3–10), dosage of adsorbent (0.1–0.7 g/L), contact time (10–80 min), process temperature (298–348 K), and nickel ion initial concentration (10–70 ppm). It is worth noting that the stirring rate was set at 200 rpm for all of the experiments.

The experiments were started by investigating the effect of pH and determining its optimal value for nickel(II) ions adsorption. To attain this goal, different samples of 100 mL Ni ions aqueous solutions in pH range of 3–10, concentration

value of 30 ppm, adsorbent dosage of 0.1 g/L, 60 min, and at room temperature were prepared and tested. When the optimized pH value was achieved, the next adsorption tests were performed at the pH optimal value. During the optimization of each parameter, the others were set in the optimal values and their significance were studied in the above mentioned ranges. After each adsorption experiment, the adsorbent was separated from the achieved solution by Whatman filter paper 42 and the residual nickel was determined using a flame atomic adsorption device. Then using Eqs. (1) and (2), the nickel ions adsorption percentage (%R) and the adsorption capacity (q_e) were determined, respectively:

$$R\,(\%) = \left(\frac{C_i - C_o}{C_i}\right) \times 100 \tag{1}$$

$$q_e = \left(\frac{C_i - C_o}{W}\right) \times V \tag{2}$$

where C_i is the initial concentration of the metal ions (mg/l), C_o is the equilibrium concentration of the metal ions (mg/l), V is the volume of solution (L), W is the weight of the dried adsorbent (g), R is the heavy metal ions adsorption percentage, and q_e is the adsorption capacity per gram of dried adsorbent (mg/g).

3 Results and Discussion

3.1 Characterization of the Adsorbent

In this study, BET analysis showed that the surface area of the adsorbent produced from the leaves of *Mespilus germanica* tree was equal to 10.39 m^2/g.

The surface variations of the current adsorbent was investigated before and after the process by SEM analysis. In order to prepare the activated carbon samples for SEM, they were coated by a thin gold layer in the vacuum condition. The SEM micrographs are presented in Fig. 1. It can be observed there are pores, ripplings, and holes on the adsorbent surface which increase its specific surface area and vacant active sites for nickel ions adsorption (Fig. 1a). Moreover, it can be clearly seen that the majority of the surface holes were occupied and covered by the adsorbed ions after the adsorption process (Fig. 1b).

XRD analysis output of the activated carbon produced from the *Mespilus germanica* leaves is shown in Fig. 2. As it can be observed there is a peak in $2\theta = 29°$ which is the characteristic of carbon and its crystalline structure. There are some other peaks in $2\theta = 23°$ and 47° which represent the dispersions of graphite structure of the activated carbon sample [15].

The effect of adsorption of nickel ions on the surface functional groups of the prepared adsorbent was studied by FTIR analysis in the spectrum range of 400–4000 $cm^{-1}$and the results are shown Fig. 3. The peak which is seen in 719.795 cm^{-1} is associated to the tension bond of –C–H aromatic functional group [16]. There are some other peaks in the wavenumbers 1017.45 cm^{-1}, 1458.01 cm^{-1}, 2923.82 cm^{-1}, 3434.42 cm^{-1}, and 3745.05 cm^{-1} which are attributed to aromatic ring, amide bonds, C–H (stretching), N–H, and H–O (alcohol) functional groups, respectively [17–21]. The changes in the FTIR spectrum after nickel ion adsorption is obvious (Fig. 3b). There is a peak in wavenumber of 481.07 cm^{-1} which is associated with C–I functional group while the peak in wavenumber of 620.48 cm^{-1} is related to N–H functional group [22, 23]. There are some other peaks in frequencies 1120.7 cm^{-1}, 1433.7 cm^{-1},

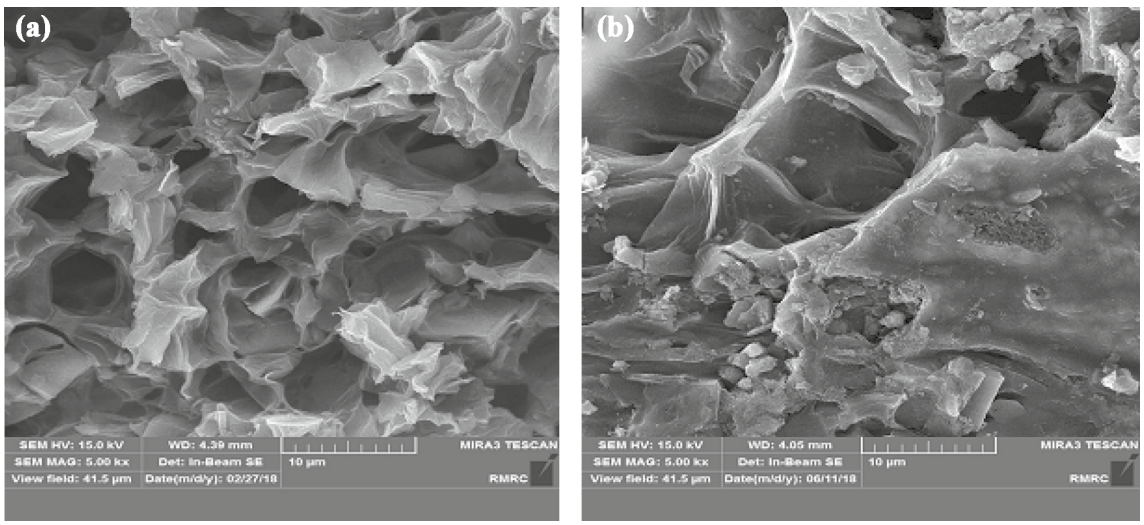

Fig. 1 SEM micrographs of the adsorbent; **a** before the adsorption and **b** after the adsorption

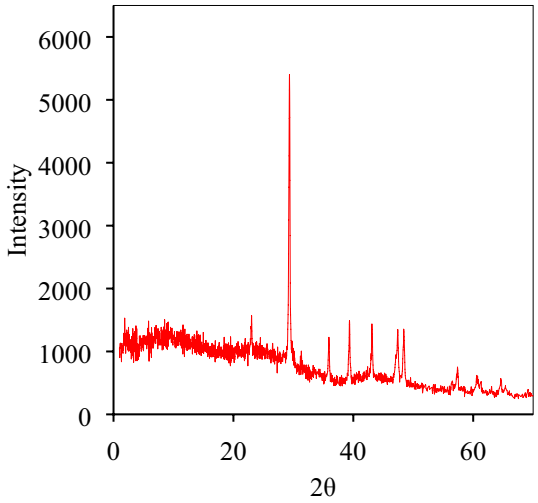

Fig. 2 XRD analysis of the produced activated carbon

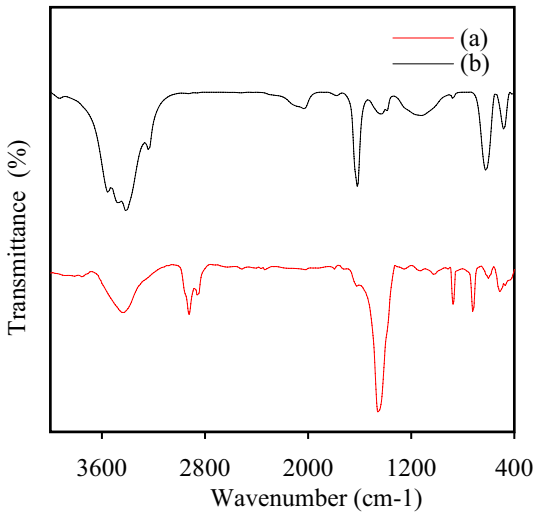

Fig. 3 FTIR diagram of the adsorbent **a** before and **b** after the adsorption process

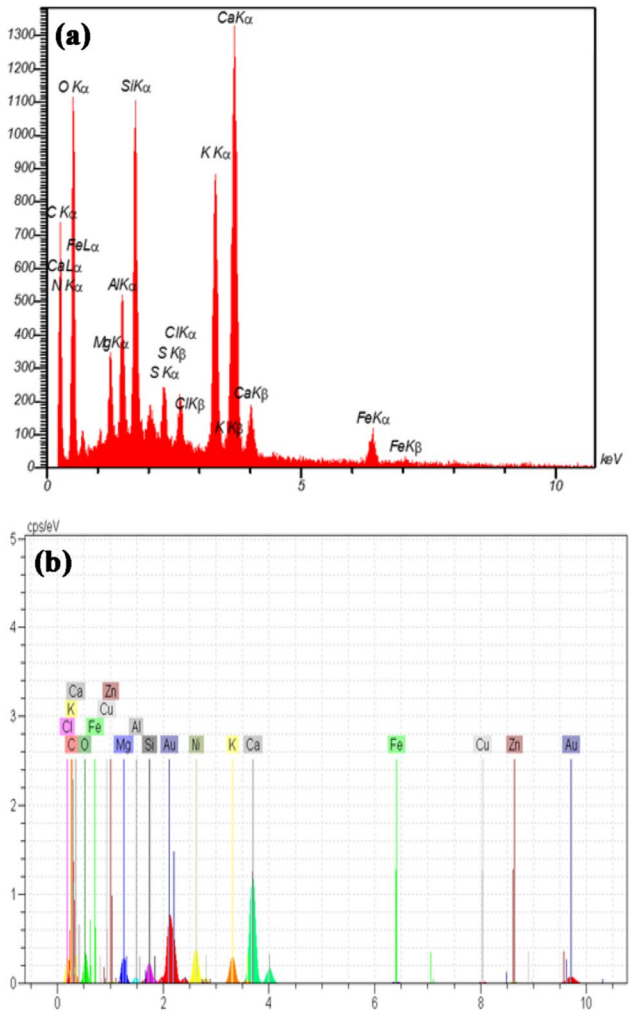

Fig. 4 Result of EDAX analysis; **a** before the adsorption and **b** after the adsorption

1617.11 cm^{-1}, 2030.69 cm^{-1}, 3236.37 cm^{-1}, 3412.12 cm^{-1}, and 3552.62 cm^{-1}, which are related to C–O, P=O, aromatic ring, $Rh^{I}(CO)2$, N–H (tensile bond), O–H, and OH (alcohol with hydrogen bond), respectively [24–30]. The most striking result to emerge from the current FTIR spectrum is that the functional groups play a major role in the adsorption process [31–33].

The other technique which was performed to characterize the produced adsorbent from the *Mespilus germanica* leaves was EDAX, and its results are presented in Fig. 4 and Table 1. Based on these data, it can be concluded that carbon and oxygen are the main constituents of the produced adsorbent before the adsorption process, since their weight percentages are 25.8 and 38.89, respectively. The other elements and their weight percentages are presented in Table 1. EDAX analysis after the adsorption process shows the presence of nickel (1.39%) on the adsorbent. Obviously carbon is the main constituent (46.97 wt%) again. It should be noted that the low value of nickel can be related to the local analysis of the elements.

3.2 Effect of Solution pH

One of the significant parameters which affects the adsorption process is the solution pH [34]. There is an intense competition between hydrogen (H^+) and other ions in the solution for adsorption on adsorbent. Additionally, pH of solution changes the adsorbent surface charge and the adsorbate (nickel ion) ionization degree during the adsorption process. In this research, solution pH was changed in the range of 3–10 and its effect on the nickel ions adsorption

Table 1 Result of EDAX analysis before the adsorption and after the adsorption

Adsorbent	Element	Wt%	Atomic %	Adsorbent	Element	Wt%	Atomic %
Before adsorption	C	25.80	37.47	After adsorption	C	46.97	66.09
	N	3.86	4.81		O	23.38	24.18
	O	38.89	42.40		Mg	1.66	1.13
	Mg	1.39	1.00		Cl	5.54	1.19
	Al	2.11	1.37		Al	0.34	0.21
	Si	4.40	2.73		Si	1.16	0.69
	S	1.22	0.66		Ni	1.39	1.12
	Cl	1.15	0.57		K	2.20	0.93
	K	6.81	3.04		Ca	10.19	4.21
	Ca	11.96	5.20		Fe	0.15	0.05
	Fe	2.39	0.75		Cu	0.29	0.08
	Total	**100.00**	**100.00**		Zn	0.39	0.10
					Au	13.84	1.16
					Total	**100.00**	**100.00**

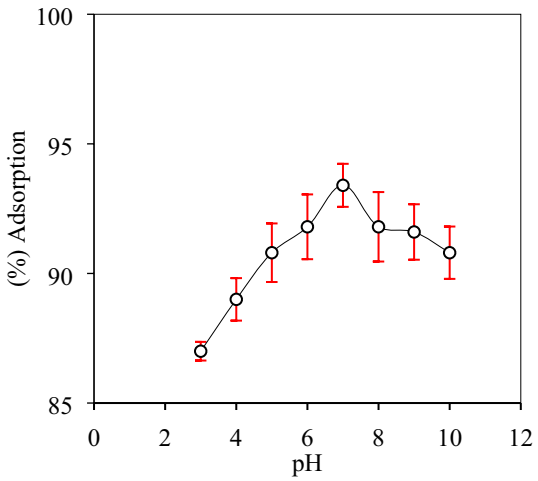

Fig. 5 Effect of solution pH on nickel ions removal percentage using the activated carbon produced from *Mespilus germanica* leaves (Ni^{2+} = 30 ppm, t_c = 60 min, m = 0.1 g/L, T = 298 K)

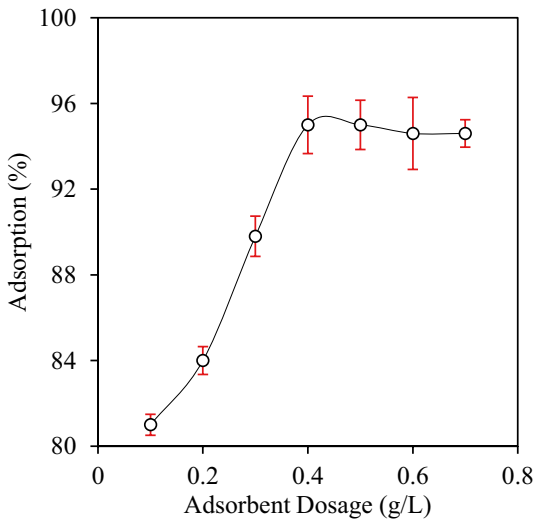

Fig. 6 The adsorbent dosage effect on nickel ions removal percentage using the activated carbon produced from the *Mespilus germanica* leaves (Ni^{2+} = 30 ppm, t_c = 60 min, pH = 7, T = 298 K)

percentage using activated carbon produced from the *Mespilus germanica* leaves is shown in Fig. 5.

As it can be obviously observed in Fig. 5, the adsorption percentage registered a rise from 87 to 93.4% when pH was changed in the range of 3–7, and it decreased after pH = 7. In low pH values the concentration of H^+ ions in the solution is so high that they overcome the other metallic cations in competition for relocating on the adsorbent surface by repulsive electrostatic interactions between H^+ cations and metallic ions [35]. In pH range of 3–7, it can be said that the lower the pH value, the lower the adsorption efficiency. In the range of alkali pH values, the adsorption percentage declined. This can be related to the removal of cations and the presence of OH^- ions in the solution and the formation of metallic hydroxides. Overall, pH = 7 is the optimum value in the current adsorption process. There are similarities between the attitudes expressed in this study and those described by Dong et al. [36] and Rathinam et al. [37].

3.3 Effect of Adsorbent Dosage

Prior studies have noted the importance of adsorbent dosage in adsorption process since the adsorption capacity of the applied adsorbent is determined in any concentration of metallic ions by this variable [38]. Figure 6 presents the effect of adsorbent dosage on removal percentage of nickel(II) ions from aqueous solution. In this figure, there is a clear trend of increase of adsorption efficiency from 81 to 95% when the adsorption dosage changed between 0.1

and 0.4 g/L. Additionally, there was not any further rise in adsorption percentage after this point. An explanation for the increase in the adsorption efficiency in the early stage of the diagram might be that the produced adsorbent's surface area and the number of active sites are so high. These findings further support the idea that says the maximum adsorption occurs in an appropriate dosage of the adsorbent and no significant adsorption was found for the residual cations after this point [39].

3.4 Effect of Contact Time

Figure 7 presents the effect of adsorption time on the adsorption efficiency of nickel heavy metal ions using the current adsorbent in the range of 10–80 min.

It is apparent from this figure that the optimum value of contact time for the adsorption of nickel is 50 min (adsorption efficiency of 97%). From the data in Fig. 7, it is clear that adsorption rate is very high in the early values of contact time. This result may be explained by the fact that the number of active sites on the adsorbent is so high when the adsorption started, therefore metallic ions locate on these sites. Consequently, the adsorption efficiency increased with time and then became constant after 50 min. The adsorption is in the equilibrium state at this point as the result of saturation of active sites by the metallic ions [40]. Overall, the contact time of 50 min is the optimum time for the current adsorption process.

3.5 Effect of Process Temperature

Process temperature is another parameter which affects the efficiency of an adsorption process, since it determines its exothermic/endothermic status. From Fig. 8, it can be seen that temperature had a negative impact on the adsorption of nickel ions in the range of 298–348 K. Therefore, it can be concluded that the process was exothermic and no chemical bonds were formed during the adsorption. There are several possible explanations for this result. One is that the adsorbed metal has the tendency of separation from the adsorbent and returning into the solution [41]. Considering this figure, in the current adsorption process the optimum temperature was 298 K, where the adsorption efficiency was 95.5%.

3.6 Effect of Ion Initial Concentration

During the adsorption process, the initial ion concentration plays a major role as a mass transfer driving force between the adsorbent and solution. The effect of this parameter on the adsorption efficiency is shown in Fig. 9. At initial concentration values, the ratio of the active sites to the nickel ion initial concentration is relatively high, and therefore they were adsorbed because of high interactions between the adsorbent and nickel ions. Additionally, a positive correlation was found between adsorption capacity (q_e) and initial nickel ion concentration. The explanation for such a trend is that the collisions of the ions and the adsorbent is so frequent which increases the diffusion into the adsorbent structure. The higher adsorption capacity can be associated to the high driving force between the solution and the solid phase.

3.7 Equilibrium Study

As an important component of the adsorption, isotherms are used to explain the interactions between the adsorbent and pollutants. In this study Langmuir and Freundlich isotherm

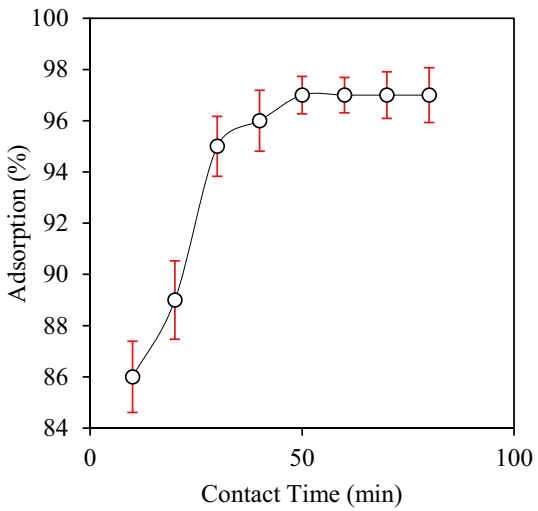

Fig. 7 The variations of adsorption percentage with contact time (Ni^{2+} = 30 ppm, pH = 7, m = 0.4 g/L, T = 298 K)

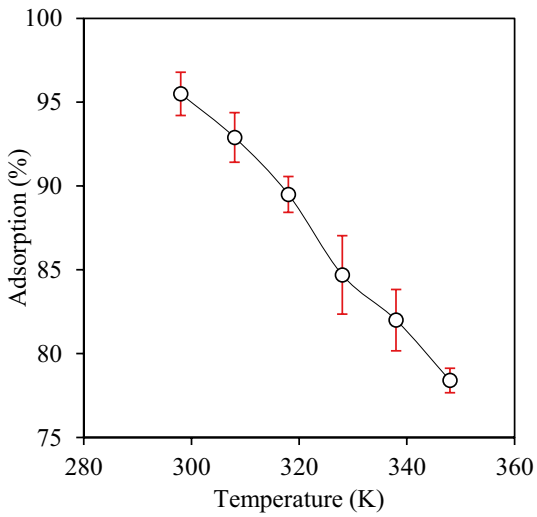

Fig. 8 The effect of process temperature on nickel ions removal percentage (Ni^{2+} = 30 ppm, pH = 7, m = 0.4 g/L, t_c = 50 min)

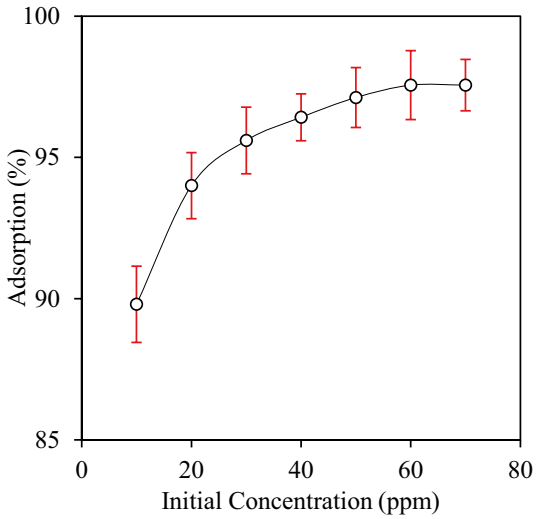

Fig. 9 The changes of nickel ions adsorption percentage with the ion initial concentration ($T = 298$ K, pH = 7, $m = 0.4$ g/L, $t_c = 50$ min)

models were applied to investigate the equilibrium behavior of nickel ions adsorption. Langmuir adsorption isotherm is used for the single-layer adsorption with finite number of surface active sites [42]. The linear form of this model is as the following:

$$\frac{1}{q_e} = \frac{1}{K_L q_m}\left(\frac{1}{C_e}\right) + \frac{1}{q_m} \tag{3}$$

As the Langmuir constants, q_m is the maximum adsorption capacity (mg/g) and K_L is the adsorption energy (L/g). In addition, q_e and C_e are the equilibrium capacity (mg/g) and the equilibrium concentration of the contaminant (mg/L). In order to calculate these constants, the slope and intercept of $1/q_e$ versus $1/C_e$ are determined. One of the principal uses of Langmuir constant is to find the adsorption intensity (R_L) using Eq. (4). For $R_L > 1$, $R_L = 0$, $R_L = 1$ and $0 < R_L < 1$, it can be said that the process is undesirable, irreversible, and linear and desirable, respectively.

$$R_L = \frac{1}{1 + K_L C_o} \tag{4}$$

Freundlich adsorption isotherm describes the adsorption processes on heterogeneous surfaces with uniform energy sites [43]. Equation (5) shows the linear form of Freundlich model:

$$\log q_e = \log K_F + \frac{1}{n}\log C_e \tag{5}$$

where K_F and n are the Freundlich isotherm constants and are used to explain the relation between the adsorption intensity and its capacity and are calculated using the slope and intercept of $\log q_e$ versus $\log C_e$. The value of constant n

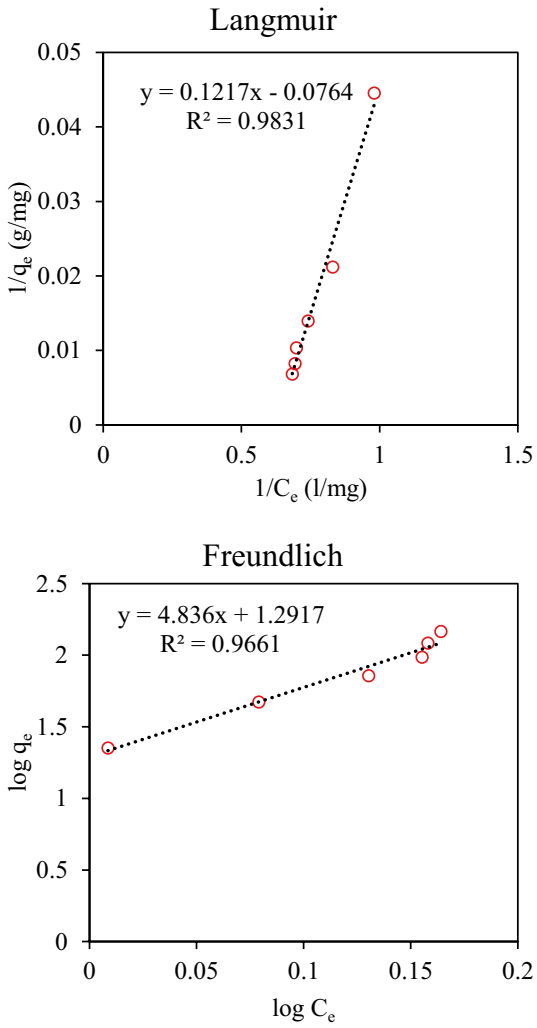

Fig. 10 The diagrams of Langmuir and Freundlich isotherms for nickel(II) ions adsorption

shows the deviation in the adsorbent behavior from the linear adsorption. If $1/n$ is between 0 and 1, adsorption is non-uniform. When it is lower and higher than 1, the process is a linear chemical and physical adsorption, respectively.

The results of the equilibrium analysis are reported in Fig. 10 and Table 2. These data illustrate some main characteristics of the current adsorption process. It is apparent from the results that Langmuir isotherm correlation coefficient (R^2) is higher than R^2 value of Freundlich model, which shows its higher capability of fitting the data and describing the isotherm behavior of nickel(II) adsorption using the activated carbon produced from the *Mespilus germanica* leaves. Additionally, it can be concluded that it is a single layer adsorption process on a homogeneous adsorbent. In addition, the value of parameter n of Freundlich model was 0.2, which suggests that the adsorption of nickel ions is physical

Table 2 Estimated parameters for Langmuir and Freundlich isotherms for the adsorption of nickel(II) ions at $m = 0.4$ g, pH = 7, $t_c = 50$ min, $T = 298$ K

Isotherm	Parameter	Value
Langmuir	q_m (mg/g)	13.08
	K_L (L/mg)	0.63
	R^2	0.9831
Freundlich	n	0.20
	K_F (mg)$^{1-n}$ L^n g^{-1}	19.54
	R^2	0.9661

and desirable. The value of q_m was 13.08 mg/g, which is comparable with the results of other researches [35].

3.8 Thermodynamic Study

The purpose of thermodynamic study is to determine parameters like enthalpy ($\Delta H°$), entropy ($\Delta S°$), and Gibbs free energy ($\Delta G°$) in order to describe the reaction equilibrium. Having the adsorption equilibrium constant (K), the thermodynamic parameters can be calculated using Eqs. (6)–(8) [44–46]:

$$K = \frac{C_{AS}}{C_A} = \frac{q_e}{C_e} \tag{6}$$

$$\Delta G° = -RT \ln K \tag{7}$$

$$\ln K = \frac{\Delta S°}{R} - \frac{\Delta H°}{RT} \tag{8}$$

In these equations R, T, and K are the universal gas constant (8.314 J/mol K), absolute temperature, and adsorption equilibrium constant, respectively. C_{AS} is the concentration of the adsorbed ion on the adsorbent surface (mg/L), while C_A is the residual ion concentration in the solution at equilibrium time (mg/L). $\Delta H°$ and $\Delta S°$ values are achieved from the slope and intercept of ln$K$ versus 1/T (Fig. 11). For $\Delta H° > 0$ the process is endothermic while it is exothermic when $\Delta H° < 0$. Considering the negative values of $\Delta H°$, $\Delta S°$, and $\Delta G°$ presented in Table 3, the current adsorption process using the activated carbon produced from the *Mespilus germanica* leaves is relatively spontaneous. Additionally, by increasing the temperature, Gibbs free energy declined, which confirms the spontaneity of the process with temperature. Based on the data in Fig. 11 and Table 3, the negative value of $\Delta H°$ (− 34.468 kJ/mol) shows that the adsorption efficiency decreased with temperature. Furthermore, it can be said that adsorption of nickel(II) ions is probably physical. Since the current process is exothermic, considering the Le Chatelier's principle, the decrease in adsorption efficiency with temperature is followed by relatively reduced irregularities.

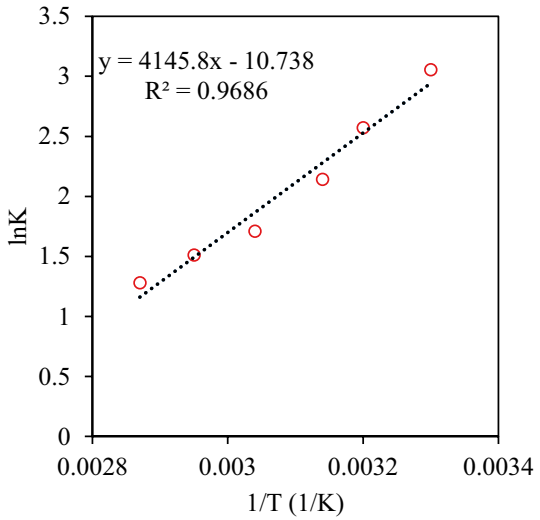

Fig. 11 Thermodynamic plot for adsorption of nickel(II) ions using activated carbon produced from the *Mespilus germanica* leaves

3.9 Kinetic Study

Since valuable information can be achieved about the reaction path and control of adsorption process through the kinetic study of the process, the study of adsorption kinetic models is of great importance [47]. In the current study the kinetic behavior of Ni(II) adsorption process is done by using pseudo-first-order and second-order kinetic models. Equations (9) and (10) show the linear form of these models, respectively [32]:

$$\ln(q_e - q_t) = \ln q_e - k_1 t \tag{9}$$

$$\frac{t}{q_t} = \frac{1}{k_2 q_e^2} + \frac{t}{q_e} \tag{10}$$

where k_1 and k_2 are the pseudo first-order and the pseudo second-order rate constants, q_t is the adsorption capacity at time t (mg/g), and t is time (min). The values of k_1 and $q_{e,cal}$

Table 3 Thermodynamic parameters of nickel(II) ions adsorption

T (K)	K	$\Delta G°$	$\Delta H°$	$\Delta S°$
298	21.2	− 7.56	− 34.468	− 89.27
308	13.08	− 6.58		
318	8.52	− 5.66		
328	5.53	− 4.66		
338	4.5	− 4.24		
348	3.63	− 3.7		

are determined by plotting the variations of $\ln(q_e - q_t)$ versus t, and k_2 and q_e are calculated from the diagram of t/q_t versus t from the pseudo second-order linear form.

The results of kinetic study of the current adsorption process are indicated in Fig. 12 and Table 4. Since the R^2 value of the pseudo second-order kinetic model (0.9997) is considerably higher than that of the pseudo-first-order kinetic model (0.9507), the former model is capable of describing the kinetics of nickel(II) ions better than the latter one. Furthermore, k_1 is lower than k_2, which mirrors the above mentioned results. Additionally, the maximum adsorption capacity calculated by the pseudo first-order kinetic model ($q_{e,cal}$) is lower than the value measured from the experimental data ($q_{e,exp}$), which confirms the weakness of this model for the description of adsorption kinetics of the current process. The maximum adsorption capacity which is calculated during the pseudo-second-order kinetic model

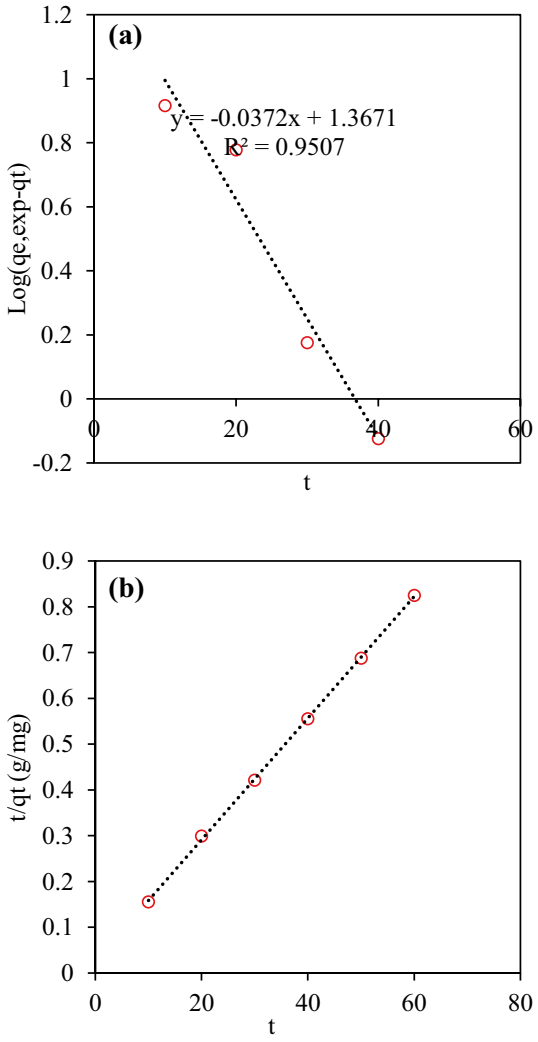

Fig. 12 Kinetic diagrams of Ni(II) adsorption process; **a** pseudo-first-order and **b** second-order kinetic model

Table 4 Kinetic parameters of nickel(II) ions adsorption o (Ni^{2+} = 60 ppm, t_c = 50 min, pH = 7, T = 298 K, m = 0.4 g)

Kinetic model	Parameter	Value
Pseudo-first-order	$q_{e,cal}$ (mg/g)	23.28
	K_1 (min^{-1})	0.1
	R^2	0.9507
Pseudo-second-order	$q_{e,cal}$ (mg/g)	75
	$K_2 \times 10^{-3}$ (g/mg min)	6.924
	R^2	0.9995
	$q_{e,exp}$ (mg/g)	72.75

analysis is 75 mg/g, which is in an acceptable accordance with the measured value. Considering these results, it can be said that pseudo-second-order kinetic model performed better than the other model in description of kinetic behavior of adsorption for nickel(II) ions using activated carbon produced from the *Mespilus germanica* leaves.

3.10 Comparison with Previous Studies

One of the goals of this study was to compare the adsorption capacity of the current adsorbent with other ones reported in the literature. Based on the data illustrated in Table 5, the maximum adsorption capacity of the activated carbon produced from the *Mespilus germanica* leaves calculated by Langmuir model was higher than the adsorbent which are based on activated carbon, although it is considerably lower than the adsorption capacity of the more complex ones.

4 Conclusions

This paper has examined the efficiency of an adsorbent prepared from *Mespilus germanica* leaves for the adsorption of nickel(II) ions from aqueous solutions. Initially, the produced activated carbon was characterized using BET, SEM, FTIR, XRD, and EDAX analyses. Thereafter the effects of operating parameters such as solution pH, adsorbent dosage, contact time, temperature, and initial concentration of nickel ions on their uptake percentage were investigated. The findings showed that the maximum adsorption efficiency which was equal to 97.56% was achieved in pH = 7, adsorbent dosage of 0.4 g/L, contact time of 50 min, temperature of 298 K, and initial ion concentration of 60 ppm. Using Langmuir and Freundlich adsorption isotherms, it was shown that the former can match the data better than the latter. Additionally, using Langmuir adsorption isotherm, the maximum adsorption capacity was calculated equal to 13.08 mg/g. Furthermore the results suggested that the adsorption of nickel(II) ions was physical. Considering the findings of the thermodynamic study, Gibbs free energy was negative, which showed

Table 5 Comparison between the maximum adsorption capacity of the current adsorbent and other adsorbents reported in the literature [35, 48–57]

References	Adsorbent	Adsorption capacity (mg/g)
[48]	Multiwalled carbon nanotubes	6.09
[49]	Macroporous Ni^{2+}-imprinted chitosan foam	69.93
[50]	Three-dimensional macroporous cellulose-based bioadsorbents	171.8
[51]	Sugarcane bagasse-derived $ZnCl_2$-activated carbon	2.99
[52]	Activated carbon prepared from cherry kernels	76.27
[53]	KOH-activated carbon from banana peel	27.4
[54]	Activated carbon	4.36
[55]	Turkish lignite	13.0
[26]	Carbon aerogel	2.80
[57]	Waste of tea factory	11.17
[35]	Bentonite/Fe_3O_4 nanocomposite	5.9808
This study	Activated carbon from *Mespilus germanica* leaf	13.08

that it was a spontaneous process. In addition, the value of ΔH° confirmed that the process was exothermic. The results of kinetic study indicated that the pseudo second-order kinetic model was more capable than the pseudo first-order model in fitting the kinetic data of adsorption for nickel(II) ions. Taken together, these results suggest that the current adsorbent can be considered as a suitable one for the treatment of wastewaters containing heavy metal ions.

References

1. Volesky, B.: Detoxification of metal-bearing effluents: biosorption for the next century. Hydrometallurgy **59**, 203–216 (2001)
2. Zahed, M.; Jafari, D.; Esfandyari, M.: Adsorption of formaldehyde from aqueous solution using activated carbon prepared from *Hibiscus rosa-sinensis*. Int. J. Environ. Anal. Chem. (2020). https://doi.org/10.1080/03067319.2020.1762872
3. Borba, C.E.; Guirardello, R.; Silva, E.A.; Veit, M.T.; Tavares, C.R.G.: Removal of nickel(II) ions from aqueous solution by biosorption in a fixed bed column: experimental and theoretical breakthrough curves. Biochem. Eng. J. **30**, 184–191 (2006)
4. Norouzi, H.; Jafari, D.; Esfandyari, M.: Study on a new adsorbent for biosorption of cadmium ion from aqueous solution by activated carbon prepared from *Ricinus communis*. Desalin. Water Treat. **191**, 140–152 (2020)
5. Eccles, H.: Removal of heavy metals from effluent streams—why select a biological process? Int. Biodeterior. Biodegrad. **35**, 5–16 (1995)
6. Habib, M.A.; Moghaddam, S.M.R.A.; Arami, M.; Hashemi, S.H.: Optimization of the electrocoagulation process for removal of Cr(VI) using Taguchi method. J. Water Wastewater **22–24**, 2–8 (2012)
7. Leyva-Ramos, R.; Diaz-Flores, P.E.; Aragon-Piña, A.; Mendoza-Barron, J.; Guerrero-Coronado, R.M.: Adsorption of cadmium(II) from an aqueous solution onto activated carbon cloth. Sep. Sci. Technol. **40**, 2079–2094 (2005)
8. Ahmedna, M.; Marshall, W.E.; Husseiny, A.A.; Rao, R.M.; Goktepe, I.: The use of nutshell carbons in drinking water filters for removal of trace metals. Water Res. **38**, 1062–1068 (2004)
9. Bouhamed, F.; Elouear, Z.; Bouzid, J.; Ouddane, B.: Multi-component adsorption of copper, nickel and zinc from aqueous solutions onto activated carbon prepared from date stones. Environ. Sci. Pollut. Res. **23**, 15801–15806 (2016)
10. Nejadshafiee, V.; Islami, M.R.: Adsorption capacity of heavy metal ions using sultone-modified magnetic activated carbon as a bio-adsorbent. Mater. Sci. Eng. C **101**, 42–52 (2019)
11. Aguayo-Villarreal, I.A.; Bonilla-Petriciolet, A.; Muñiz-Valencia, R.: Preparation of activated carbons from pecan nutshell and their application in the antagonistic adsorption of heavy metal ions. J. Mol. Liq. **230**, 686–695 (2017)
12. Yunus, Z.M.; Al-Gheethi, A.; Othman, N.; Hamdan, R.; Ruslan, N.N.: Removal of heavy metals from mining effluents in tile and electroplating industries using honeydew peel activated carbon: a microstructure and techno-economic analysis. J. Clean. Prod. **251**, 119738 (2020)
13. Aboli, E.; Jafari, D.; Esmaeili, H.: Heavy metal ions (lead, cobalt, and nickel) biosorption from aqueous solution onto activated carbon prepared from *Citrus limetta* leaves. Carbon Lett. **30**, 683–698 (2020)
14. Kyzas, G.Z.; Deliyanni, E.A.; Matis, K.A.: Activated carbons produced by pyrolysis of waste potato peels: cobalt ions removal by adsorption. Colloids Surf. A Physicochem. Eng. Asp. **490**, 74–83 (2016)
15. Yao, S.; Zhang, J.; Shen, D.; Xiao, R.; Gu, S.; Zhao, M.; Liang, J.: Removal of Pb(II) from water by the activated carbon modified by nitric acid under microwave heating. J. Colloid Interface Sci. **463**, 118–127 (2016)
16. Hamzah, M.; Khenfouch, M.; Rjeb, A.; Sayouri, S.; Houssaini, D.S.; Darhouri, M.; Srinivasu, V.V.: Surface chemistry changes and microstructure evaluation of low density nanocluster polyethylene under natural weathering: a spectroscopic investigation. IOP Conf. Ser. J. Phys. Conf. Ser. **984**, 012010 (2018)
17. Gómez-Sánchez, E.; Simon, S.; Koch, L.C.; Wiedmann, A.; Weber, T.; Mengel, M.: Atr-FTIR spectroscopy for the characterisation of magnetic tape materials. e-Preserv. Sci. **7**, 2–9 (2010)
18. Park, S.N.; Park, J.; Kim, H.O.; Song, M.J.; Suh, H.: Characterization of porous collagen/hyaluronic acid scaffold modified by

1-ethyl-3-(3-dimethylaminopropyl) carbodiimide cross-linking. Biomaterials **23**(4), 1205–1212 (2002)
19. Vidale, M.; Craig, O.; Desset, F.; Guida, G.; Bianchetti, P.; Sidoti, G.; Mariottini, M.; Battistella, E.: A chlorite container found on the surface of Shahdad (Kerman, Iran) and its cosmetic content. J. Brit. Inst. Perss. Stud. **50**(1), 27–44 (2012)
20. Ramamurthy, N.; Kannan, S.: Fourier transform infrared spectroscopic analysis of a plant (*Calotropis gigantea* Linn) from an Industrial Village, Cuddalore Dt, Tamilnadu, India. Rom. J. Biophys. **17**(4), 269–276 (2007)
21. Gabrienko, A.A.; Danilova, I.G.; Arzumanov, S.S.; Toktarev, A.V.; Freude, D.; Stepanov, A.G.: Strong acidity of silanol groups of zeolite beta: evidence from the studies by IR spectroscopy of adsorbed CO and 1 H MAS NMR. Microporous Mesoporous Mater. **131**, 210–216 (2010)
22. Sergeeva, A.V.; Zhitova, E.S.; Nuzhdaev, A.A.; Zolotarev, A.A.; Bocharov, V.N.; Ismagilova, R.M.: Infrared and Raman spectroscopy of ammoniovoltaite, $(NH_4)_2Fe^{2+}{}_5Fe^{3+}{}_3Al(SO_4)_{12}(H_2O)_{18}$. Minerals **10**(9), 781 (2020)
23. Zhuang, J.; Li, M.; Pu, Y.; Ragauskas, A.J.; Yoo, C.G.: Observation of potential contaminants in processed biomass using Fourier transform infrared spectroscopy. Appl. Sci. **10**, 4345 (2020)
24. Lewis, P.D.; Lewis, K.E.; Ghosal, R.; Bayliss, S.; Lloyd, A.J.; Wills, J.; Godfrey, R.; Kloer, P.; Mur, L.A.J.: Evaluation of FTIR spectroscopy as a diagnostic tool for lung cancer using sputum. BMC Cancer **10**, 640 (2010)
25. Hoffmann, G.; Veszpremi, T.; Nagy, A.: Properties of IR spectra of phosphorus doped SiO_2 films. Period. Polytech. Chem. Eng. Hun Da **23**(3), 175–184 (1979)
26. Melniciuc, P.N.; Pui, A.; Florescu, M.: FTIR spectroscopy for the analysis of vegetable tanned ancient leather. Eur. J. Sci. Theol. **2**(4), 49–53 (2006)
27. Basile, F.; Bersani, I.; Del Gallo, P.; Fiorilli, S.; Fornasari, G.; Gary, D.; Mortera, R.; Onida, B.; Vaccari, A.: In situ IR characterization of CO interacting with Rh nanoparticles obtained by calcination and reduction of hydrotalcite-type precursors. Int. J. Spectrosc. (2011). https://doi.org/10.1155/2011/458089
28. Kadhim, A.J.: Synthesis and characterization benzimidazole ring by using O-phenylinediamine with different compounds and using mannich reaction to preparation some of derivatives. Orient. J. Chem. **34**(1), 473–481 (2018)
29. Gipson, K.; Stevens, K.; Brown, P.; Ballato, J.: Infrared spectroscopic characterization of photoluminescent polymer nanocomposites. Spectrosc. Mater. Chem. (2015). https://doi.org/10.1155/2015/489162
30. Veiderma, M.; Knubovets, R.; Tönsuaadu, K.: Structural properties of apatites from Finland studied by FTIR spectroscopy. Bull. Geol. Soc. Finl. **70**, 69–75 (1998)
31. Gupta, V.K.; Nayak, A.; Agarwal, S.; Chaudhary, M.; Tyagi, I.: Removal of Ni(II) ions from water using scrap tire. J. Mol. Liq. **190**, 215–222 (2014)
32. Rao, M.M.; Ramana, D.K.; Seshaiah, K.; Wang, M.C.; Chien, S.W.C.: Removal of some metal ions by activated carbon prepared from *Phaseolus aureus* hulls. J. Hazard. Mater. **166**, 1006–1013 (2009)
33. Saleh, T.A.; Alhooshani, K.R.; Abdelbassit, M.S.A.: Evaluation of AC/ZnO composite for sorption of dichloromethane, trichloromethane and carbon tetrachloride: kinetics and isotherms. J. Taiwan Inst. Chem. Eng. **55**, 159–169 (2015)
34. Kong, J.; Yue, Q.; Sun, S.; Gao, B.; Kan, Y.; Li, Q.; Wang, Y.: Adsorption of Pb(II) from aqueous solution using keratin waste–hide waste: equilibrium, kinetic and thermodynamic modeling studies. Chem. Eng. J. **241**, 393–400 (2014)
35. Ahmadi, F.; Esmaeili, H.: Chemically modified bentonite/Fe_3O_4 nanocomposite for Pb(II), Cd(II), and Ni(II) removal from synthetic wastewater. Desalin. Water Treat. **110**, 154–167 (2018)
36. Dong, L.; Zhu, Z.; Ma, H.; Qiu, Y.; Zhao, J.: Simultaneous adsorption of lead and cadmium on MnO_2-loaded resin. J. Environ. Sci. **22**, 225–229 (2010)
37. Rathinam, A.; Maharshi, B.; Janardhanan, S.K.; Jonnalagadda, R.R.; Nair, B.U.: Biosorption of cadmium metal ion from simulated wastewaters using *Hypnea valentiae* biomass: a kinetic and thermodynamic study. Bioresour. Technol. **101**, 1466–1470 (2010)
38. Teimouri, A.; Esmaeili, H.; Foroutan, R.; Ramavandi, B.: Adsorptive performance of calcined *Cardita bicolor* for attenuating Hg(II) and As(III) from synthetic and real wastewaters. Korean J. Chem. Eng. **35**, 479–488 (2018)
39. Foroutan, R.; Khoo, F.S.; Ramavandi, B.; Abbasi, S.: Heavy metals removal from synthetic and shipyard wastewater using *Phoenix dactylifera* activated carbon. Desalin. Water Treat. **82**, 146–156 (2017)
40. Gusain, D.; Srivastava, V.; Sharma, Y.C.: Kinetic and thermodynamic studies on the removal of Cu(II) ions from aqueous solutions by adsorption on modified sand. J. Ind. Eng. Chem. **20**, 841–847 (2014)
41. Guyo, U.; Mhonyera, J.; Moyo, M.: Pb(II) adsorption from aqueous solutions by raw and treated biomass of maize stover—a comparative study. Process Saf. Environ. Prot. **93**, 192–200 (2015)
42. Rangabhashiyam, S.; Selvaraju, N.: Adsorptive remediation of hexavalent chromium from synthetic wastewater by a natural and $ZnCl_2$ activated *Sterculia guttata* shell. J. Mol. Liq. **207**, 39–49 (2015)
43. Kizilkaya, B.; Tekinay, A.A.; Dilgin, Y.: Adsorption and removal of Cu(II) ions from aqueous solution using pretreated fish bones. Desalination **264**, 37–47 (2010)
44. Lee, K.J.; Miyawaki, J.; Shiratori, N.; Yoon, S.-H.; Jang, J.: Toward an effective adsorbent for polar pollutants: formaldehyde adsorption by activated carbon. J. Hazard. Mater. **260**, 82–88 (2013)
45. Mehrizad, A.; Aghaie, M.; Gharbani, P.; Dastmalchi, S.; Monajjemi, M.; Zare, K.: Comparison of 4-chloro-2-nitrophenol adsorption on single-walled and multi-walled carbon nanotubes. Iran. J. Environ. Health Sci. Eng. **9**, 5 (2012)
46. Sivakumar, S.; Muthirulan, P.; Sundaram, M.M.: Adsorption kinetic and isotherm studies of Azure A on various activated carbons derived from agricultural wastes. Arab. J. Chem. **12**, 1507–1514 (2019)
47. Özer, A.; Pirincci, H.B.: The adsorption of Cd(II) ions on sulphuric acid-treated wheat bran. J. Hazard. Mater. **137**, 849–855 (2006)
48. Abdel-Ghani, N.T.; El-Chaghaby, G.A.; Helal, F.S.: Individual and competitive adsorption of phenol and nickel onto multiwalled carbon nanotubes. J. Adv. Res. **6**(3), 405–415 (2015)
49. Guo, N.; Su, S.; Liao, B.; Ding, S.; Sun, W.: Preparation and properties of a novel macro porous Ni^{2+}-imprinted chitosan foam adsorbents for adsorption of nickel ions from aqueous solution. Carbohydr. Polym. **165**, 376–383 (2017)
50. Liu, L.; Xie, J.P.; Li, Y.J.; Zhang, Q.; Yao, J.M.: Three-dimensional macroporous cellulose-based bioadsorbents for efficient removal of nickel ions from aqueous solution. Cellulose **23**, 723–736 (2016)
51. Tran, T.V.; Bui, Q.T.P.; Nguyen, T.D.H.; Le, N.T.; Bach, L.G.: A comparative study on the removal efficiency of metal ions (Cu^{2+}, Ni^{2+}, and Pb^{2+}) using sugarcane bagasse-derived $ZnCl_2$-activated carbon by the response surface methodology. Adsorpt. Sci. Technol. **35**, 72–85 (2017)

52. Pap, S.; Radonić, J.; Trifunović, S.; Adamović, D.; Mihajlović, I.; Miloradov, M.V.; Sekulića, M.T.: Evaluation of the adsorption potential of eco-friendly activated carbon prepared from cherry kernels for the removal of Pb^{2+}, Cd^{2+} and Ni^{2+} from aqueous wastes. J. Environ. Manag. **184**, 297–306 (2016)
53. Thuan, T.V.; Quynh, B.T.P.; Nguyen, T.D.; Ho, V.T.T.; Bach, L.G.: Response surface methodology approach for optimization of Cu^{2+}, Ni^{2+} and Pb^{2+} adsorption using KOH-activated carbon from banana peel. Surf. Interfaces **6**, 209–217 (2017)
54. Keränen, A.; Leiviskä, T.; Salakka, A.; Tanskanen, J.: Removal of nickel and vanadium from ammoniacal industrial wastewater by ion exchange and adsorption on activated carbon. Desalin. Water Treat. **53**, 2645–2654 (2015)
55. Pehlivan, E.; Arslan, G.: Removal of metal ions using lignite in aqueous solutiondlow cost biosorbents. Fuel Process. Technol. **88**, 99–106 (2007)
56. Goel, J.; Kadirvelu, K.; Rajagopal, C.; Garg, V.K.: Investigation of adsorption of lead, mercury and nickel from aqueous solutions onto carbon aerogel. J. Chem. Technol. Biotechnol. **80**, 469–476 (2005)
57. Malkoc, E.; Nuhoglu, Y.: Removal of Ni(II) ions from aqueous solutions using waste of tea factory: adsorption on a fixed-bed column. J. Hazard. Mater. **135**, 328–336 (2006)